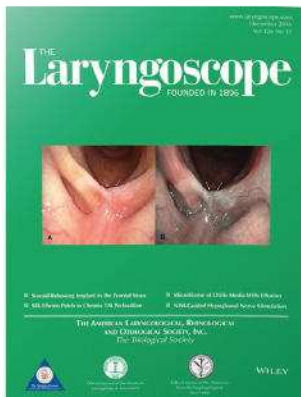


# Premiere Publications from The Triological Society

Read all three of our prestigious publications, each offering high-quality content to keep you informed with the latest developments in the field.

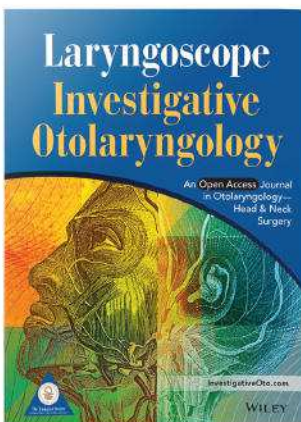


## THE Laryngoscope FOUNDED IN 1896

Editor-in-Chief: Michael G. Stewart, MD, MPH

The leading source for information  
in head and neck disorders.

[Laryngoscope.com](http://Laryngoscope.com)

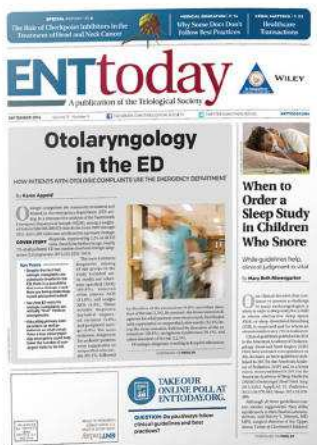


## Laryngoscope Investigative Otolaryngology Open Access

Editor-in-Chief: D. Bradley Welling, MD, PhD, FACS

Rapid dissemination of the science and practice  
of otolaryngology-head and neck surgery.

[InvestigativeOto.com](http://InvestigativeOto.com)



## ENTtoday A publication of the Triological Society

Editor-in-Chief: Alexander Chiu, MD

Must-have timely information that Otolaryngologist-head and neck surgeons can use in daily practice.

[Enttoday.org](http://Enttoday.org)

WILEY

# Growth of Benign and Malignant Schwannoma Xenografts in Severe Combined Immunodeficiency Mice

Long-Sheng Chang, PhD; Jacob Abraham, MD; Mark Lorenz, MD; Jonathan Rock, BS;  
Elena M. Akhmametyeva, MD, PhD; Georgeta Mihai, MS; Petra Schmalbrock, PhD;  
Abhik R. Chaudhury, MD; Raul Lopez, BS; Jyoji Yamate, PhD; Markus R. John, PhD;  
Hannes Wickert, PhD; Brian A. Neff, MD; Edward Dodson, MD; D. Bradley Welling, MD, PhD

**Objectives:** Models for the development of new treatment options in vestibular schwannoma (VS) treatment are lacking. The purpose of this study is to establish a quantifiable human VS xenograft model in mice. **Study Design and Methods:** Both rat malignant schwannoma cells (KE-F11 and RT4) and human malignant schwannoma (HMS-97) cells were implanted near the sciatic nerve in the thigh of severe combined immunodeficiency (SCID) mice. Additionally, human benign VS specimens were implanted in another set of SCID mice. Three-dimensional tumor volumes were calculated from magnetic resonance images over the next 6 months. **Results:** Mice implanted with malignant schwannoma cells developed visible tumors within 2 weeks. Imaging using a 4.7-tesla magnetic resonance imaging and immunohistopathologic examination identified solid tumors in all KE-F11 and HMS-97 xenografts, whereas RT4 xenografts consistently developed cystic schwannomas. VS xenografts demonstrated variability in their growth rates similar to human VS. The majority of VS xenografts did not grow but persisted throughout the study, whereas two of 15 xenografts grew significantly. Histopathologic examination and immunohistochemistry con-

firmed that VS xenografts retained their original microscopic and immunohistochemical characteristics after prolonged implantation. **Conclusions:** This study describes the first animal model for cystic schwannomas. Also, we demonstrate the use of high-field magnetic resonance imaging to quantify VS xenograft growth over time. The VS xenografts represent a model complimentary to *Nf2* transgenic and knockout mice for translational VS research. **Key Words:** Vestibular schwannoma, neurofibromatosis type 2 (NF2), xenograft, severe combined immunodeficiency (SCID) mice, magnetic resonance imaging (MRI), cystic, malignant, gadolinium.

*Laryngoscope*, 116:2018–2026, 2006

## INTRODUCTION

Vestibular schwannomas (VS) have no known medical therapies available. However, significant morbidity, including hearing loss and facial weakness, remain major concerns. VS can be divided into four general categories, including unilateral sporadic VS, neurofibromatosis type 2 (NF2)-associated VS, cystic, and malignant schwannomas.<sup>1</sup> Among VS, sporadic unilateral solid tumors are by far the most common, occurring in 10 to 13 persons per million per year. The development of bilateral VS is the hallmark of NF2, an autosomal-dominant disease caused by mutations in the neurofibromatosis type 2 (NF2) gene on chromosome 22q12.<sup>2,3</sup> Most of these solid tumors, either sporadic or NF2-associated, grow at a slow rate of approximately 1 to 2 mm per year.<sup>1</sup> Cystic schwannomas are a particularly aggressive group of unilateral schwannomas. They invade the surrounding cranial nerves, splaying them throughout the tumor.<sup>4</sup> Cystic tumors may grow rapidly and are typically more difficult to manage, often resulting in hearing loss and facial nerve paralysis on their removal.<sup>5</sup> In addition to NF2-associated tumors, mutations in the NF2 gene have been detected in sporadic VS and cystic schwannomas.<sup>6</sup> The most aggressive and rare variant is the malignant VS or triton tumor. These

From the Departments of Pediatrics (L.-S.C., E.M.A.), Otolaryngology (L.-S.C., J.A., B.A.N., E.D., D.B.W.), Pathology (L.-S.C., A.R.C.), and Radiology (G.M., P.S.), The Ohio State University and the College of Medicine (L.-S.C., M.L., J.R., P.S., A.R.C., R.L., E.D., D.B.W.), Columbus, Ohio, U.S.A.; the Center for Childhood Cancer (L.-S.C., E.M.A.), Children's Research Institute, Columbus, Ohio, U.S.A.; Laboratory of Veterinary Pathology (J.Y.), Osaka Prefecture University, Osaka, Japan; Musculoskeletal Diseases Exploratory Clinical Development Unit (M.R.J.), Novartis Pharma AG, Basel, Switzerland; and Hygiene Institut (H.W.), Abteilung Parasitologie, Universitätsklinikum Heidelberg, Heidelberg, Germany.

Editor's Note: This Manuscript was accepted for publication July 18, 2006.

Supported by grants from the U.S. Department of Defense NF Research Program and National Institute of Deafness and Communication Disorders.

Send correspondence to Long-Sheng Chang, Children's Hospital and Department of Pediatrics, The Ohio State University, 700 Children's Drive, Columbus, OH 43205. E-mail: lchang@chi.osu.edu

DOI: 10.1097/01.mlg.0000240185.14224.7d



malignant tumors occur either sporadically or after radiation and are uniformly fatal.<sup>7</sup>

Magnetic resonance imaging (MRI) distinguishes clearly among the various types of VS. Cystic regions within cystic schwannomas are signal intense on T2-weighted images, whereas noncystic components of these tumors enhance on T1-weighted images with gadolinium (Gd) in a manner similar to those seen in sporadic and NF2-associated VS.<sup>1</sup> These represent a unique tumor type clinically and histologically and should not be confused with degenerative regions of larger tumors. The irregular appearance of some heterogeneous tumors on contrast-enhanced T1-weighted images may be accounted for by hemosiderin deposits, which correlates with increasing tumor size,<sup>8</sup> but these tumors do not contain fluid as demonstrated on T2 imaging. Although distinct clinically and by MRI, the underlying molecular differences among the three benign types of VS are not understood. Malignant schwannomas invade surrounding tissues locally and progress rapidly.<sup>7</sup> Most appear solid and enhance on T1-weighted images but lack the capsule of the more common benign VS. Additionally, the optimal treatment regimen for each subtype of VS is not known because of a lack of understanding of fundamental tumor biology and a lack of rigorous clinical outcome studies.

Several studies previously attempted to implant human VS tissues in immunodeficient mice. Lee et al.<sup>9</sup> implanted human schwannomas in nude mice and showed that the tumors grew most consistently when placed in the sciatic nerve region. Charabi et al.<sup>10</sup> and Stidham et al.<sup>11</sup> confirmed that VS tissues could be successfully implanted and maintained in a subcutaneous pocket of nude mice. Although these studies demonstrated macroscopic growth in some of the transplanted VS tissues, an effective means of assessing the survival, growth, and blood supply of tumor xenografts was lacking. In addition, no study to date has compared the growth potential of various types of schwannoma tissues in mice.

We evaluated the growth characteristics of rodent and human malignant schwannoma cells as well as benign human VS xenografts in severe combined immunodeficiency (SCID) mice using a 4.7-T MRI. Our results demonstrated the feasibility of using MRI to quantify VS xenografts in mice. Interestingly, MRI also distinguished two different schwannoma types, which were confirmed by immuno- and histopathologic analysis.

## MATERIALS AND METHODS

### Experimental Design

The Institutional Animal Care and Use Committee of The Ohio State University approved the animal protocols used in this study. Healthy female SCID mice (Harlan Co., Indianapolis, IN) were housed according to approved procedures. The first series of experiments involved injecting three groups of SCID mice subcutaneously in the thigh with rat malignant schwannoma cells KE-F11<sup>12</sup> and RT4<sup>13</sup> as well as human malignant schwannoma HMS-97 cells.<sup>14</sup> Tumor growth was observed over 4 weeks and measured using a 4.7-T small-animal MRI scanner (Bruker, Billerica, MA). After euthanizing the animals, specimens were harvested for histopathologic analysis. A second set of experiments was performed using human VS specimens. SCID mice were

implanted with VS tissues obtained directly from patients undergoing surgical resection. All VS implants were placed in the proximal thigh of the left leg near the sciatic nerve. Tumor growth, if any, was accessed serially by MRI over the subsequent months after xenotransplantation. Histopathologic examination and immunohistochemical analysis were also performed on selected mice to confirm the imaged regions contain viable tumor rather than scar tissues.

### Tissue Procurement

A human subject protocol for the acquisition and analysis of human vestibular schwannomas was approved by our Institutional Reviewed Board. Patient consents were obtained before surgery. Each tumor specimen was confirmed by a pathologist as schwannoma. For implantation of human VS tissues into SCID mice, freshly removed specimen was placed in a sterile tube containing Dulbecco modified minimum essential (DME) medium (Invitrogen, Carlsbad, CA) and transported immediately to the animal research facility. Also, a portion of tumor was snap-frozen in liquid nitrogen for future molecular studies.

### Growth of Schwannoma Cells

Rat malignant schwannoma KE-F11 and RT4 cells and human malignant schwannoma HMS-97 cells were grown in DME medium supplemented with 10% fetal bovine serum (Invitrogen). For inoculation of rat KE-F11 or RT4 cells into each SCID mouse,  $2.5 \times 10^5$  cells were washed with phosphate-buffered saline and suspended in 0.2 mL of Matrigel (BD Biosciences, San Jose, CA). For inoculation of human HMS-97 cells into each SCID mouse,  $5 \times 10^5$  cells were used.

### Injection Technique

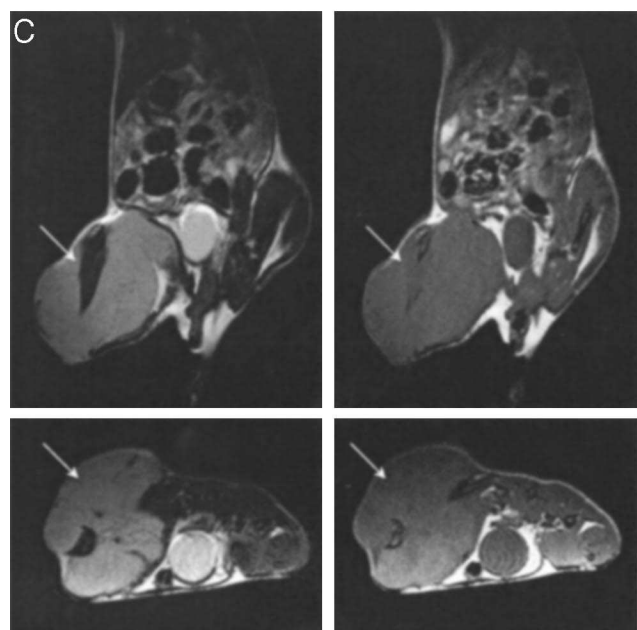
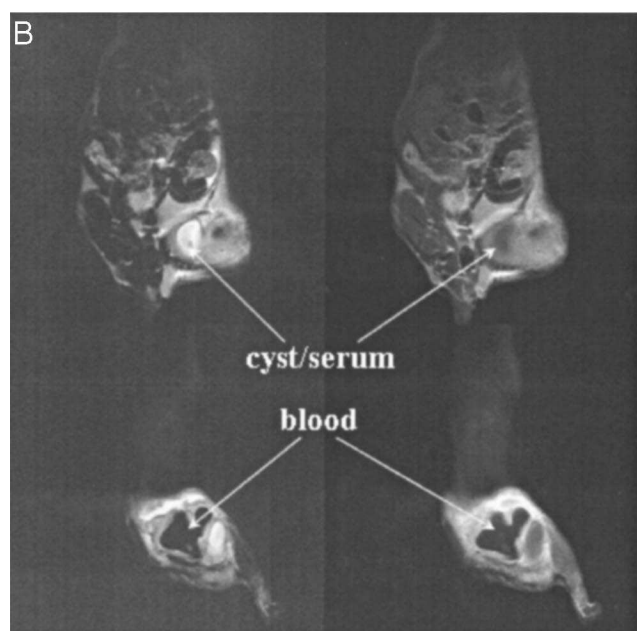
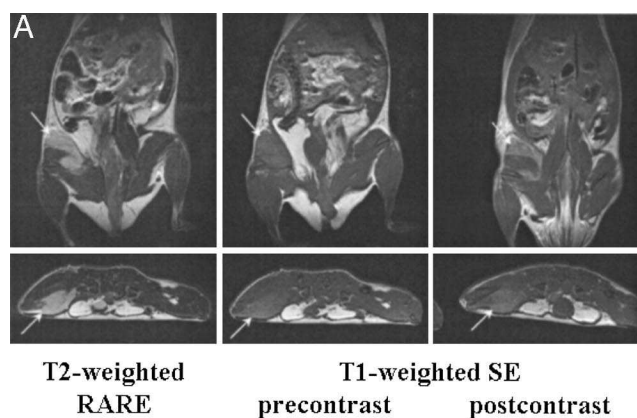
SCID mice were anesthetized by intraperitoneal injection of Avertin (2,2,2-tribromoethanol + tert-amyl alcohol; Sigma-Aldrich, St. Louis, MO) or by isoflurane inhalation. Under anesthesia, the left flank of mouse was shaved and prepped using aseptic technique. An 18-gauge needle was used to inject 0.2 mL of schwannoma cells 3 mm inferior to the greater trochanter of femur. The thigh was selected for ease of implantation and the ability to grossly observe tumor growth. Additionally, previous studies indicated that proximity to a peripheral nerve might affect growth.<sup>9–11</sup> Injected mice were revived on a warming blanket until recovery and were watched daily for tumor growth.

### Surgical Implantation Technique

An incision was made along the long axis of the proximal thigh. The contralateral leg was not dissected and used as a control for imaging. Soft tissues were dissected bluntly to identify the biceps femoris muscle and the sciatic nerve. A piece of VS tumor specimen (1–5 mm in diameter) was implanted en bloc near the nerve and the skin was closed using a single layer of interrupted suture.

### Magnetic Resonance Imaging

Mice were anesthetized with Avertin, immobilized on an animal holder, and placed prone in a 4.7-T/cm MRI system with a 120-mm inner diameter gradient coil (maximum 400 mT/m), a 72-mm inner diameter proton volume radiofrequency coil for transmit, and a 4-cm surface receive coil. For T1-weighted axial and coronal images, a spin echo sequence with TR of 550 to 600 ms and TE of 10.5 ms was used. For T2-weighted images, a rapid acquisition with refocusing echoes (RARE) sequence with TR of 2500 to 2600 ms, an effective TE of 47 to 54 ms, and a RARE factor of 4 was used. In-plane resolution was 156  $\mu$ m on the axial and 195  $\mu$ m on the coronal images, and the slice thickness was 0.8



mm with a 0.2-mm gap between slices. Scan time was 5 to 6 minutes per scan.

In addition, contrast-enhanced T1 axial and coronal images were acquired after a bolus injection with Gadodiamide (Omniscan; GE Health Care, Piscataway, NJ; 0.1-mL bolus of 10 mmol/L). The contrast agent was injected through a tail vein catheter using thin polyethylene tubing that reached outside the magnet and allowed quick delivery of the contrast agent without changing the position of the mouse inside the magnet. Mice with rat schwannoma cell implants were imaged within 2 weeks of implantation and those with human schwannoma cell implants were imaged approximately 4 weeks after inoculation. Mice with human VS implants were imaged at indicated times over the course of a year postprocedure.

Multiplanar tumor volumes were determined from T1- and T2-weighted images. For these measurements, tumor areas were manually traced on axial and coronal T1 and T2 images. Postcontrast images were also used when available. Tumor volumes were calculated by adding the traced areas from all slices depicting the tumor and multiplying with the distance between slice (i.e., 0.8-mm slice thickness + 0.2-mm gap = 1 mm). Tumor volumes measured from axial and coronal or T1 and T2 images were in fair agreement. All volume measurements were referenced to the first MRIs taken 1 month after implantation.

### Immunohistopathologic Analysis

Tumors grown in mice with schwannoma xenografts were dissected, fixed in 10% buffered formalin, and embedded in paraffin. Five-micron tissue sections were mounted, deparaffinized, and processed for standard hematoxylin–eosin staining or immunostaining with antibodies against S-100 protein (1:200 dilution of anti-S-100 from Dako, Carpinteria, CA), myelin basic protein (MBP) (prediluted anti-MBP from Zymed, San Francisco, CA), and NGF-receptor (p75<sup>NGFR</sup>)/neurotrophin receptor (1:100 dilution of anti-p75<sup>NGFR</sup> from LabVision/NeoMarker, Fremont, CA) according to previously described procedures.<sup>6</sup> A hematoxylin counterstain was then applied and the stained tissue visualized by light microscopy. Negative controls were treated with the same immunostaining procedure except without the primary antibody.

### RESULTS

KE-F11 and HMS-97 schwannoma xenografts developed solid tumor phenotypes, whereas RT4 xenografts produced cystic tumors. SCID mice injected with either the KE-F11 or RT4 rat malignant schwannoma cells produced visible tumors within 1 week after inoculation. On the MRI obtained within 2 weeks of xenotransplantation, the two sets of mice demonstrated significantly different imaging characteristics. All mice implanted with KE-F11

Fig. 1. Magnetic resonance imaging scans of malignant schwannoma xenograft 2 weeks after implantation display the presence of solid tumor mass in the left thigh (arrow). The T2-weighted rapid acquisition with refocusing echoes images (left) and T1-weighted images without (middle) and with contrast agent (right) were obtained according to "Methods." The tumor is seen hyperintense to muscle on T2 and isointense on T1 images and enhances after the injection of contrast agent (arrows). (B) Coronal (top) and axial (bottom) images of a rat RT4 schwannoma xenograft 2 weeks after implantation show the presence of a cystic tumor. Blood appeared hypointense in signal intensity on both T1 and T2 images, whereas the cyst was hyperintense on T2 images (left) and dark on T1 images (right). (C) Magnetic resonance images of a human HMS-97 schwannoma xenograft 4 weeks after implantation demonstrating a large tumor with solid architecture.



cells developed solid tumors, and the presence of tumor created significant asymmetry in the implanted thigh (Fig. 1A). Coronal and axial T2-weighted RARE images showed that the tumor mass appeared homogenous but was hyperintense or brighter to the surrounding musculature. On T1-weighted images, the tumor-containing region was near isointense to muscle and enhanced on post-contrast T1 images (arrows) as is characteristics of human VS tissues *in situ*. In contrast, all mice injected with RT4 cells demonstrated a distinctive cystic phenotype (Fig. 1B). Within the tumor mass, blood-filled cavities appeared darkest on both T1- and T2-weighted images, whereas the cysts displayed high signal intensity on T2 images but were dark on T1 images. Similar to the KE-F11 xenografts, MRIs revealed that all mice with human malignant schwannoma HMS-97 implants developed large, homogenous, solid tumors by 4 weeks postimplantation as seen on coronal and axial T1- and T2-weighted images (Fig. 1C). There were no cystic changes.

To confirm that the xenografts retained their schwannoma phenotype, histopathologic examination was performed on tumor-bearing mice. No metastatic lesions were found. Macroscopic and microscopic analysis confirmed the solid phenotype for both the KE-F11 and HMS-97 tumors and the cystic phenotype for the RT4 xenografts (Fig. 2). The KE-F11 cell line was derived from a spontaneous malignant schwannoma found in an aged male F344 rat.<sup>12</sup> The KE-F11 xenograft was a grayish, creamy globoid mass, which histologically consisted of actively growing, heterochromatic, oval- or spindle-shaped cells with large pleomorphic nuclei (Fig. 2A). RT4 is a clonal schwannoma cell line derived from a peripheral nervous system tumor induced by ethylnitrosourea injection in a newborn BDIX rat.<sup>13</sup> The xenograft generated by RT4 cells contained multiple cysts; some of the cysts contained dark, viscous blood products, whereas others were filled with serous fluid. Histologically, the RT4 tumor contained compact spindle cells with a high nucleus to cytoplasm ratio and had increased perivascular cellularity (Fig. 2B). The HMS-97 cell line was established from a malignant schwannoma from an adult patient with oncogenic osteomalacia.<sup>14</sup> Similar to KE-F11, the HMS-97 tumor was a large globoid mass comprised of heterochromatic ovoid cells with multiple mitotic figures (Fig. 2C). The HMS-97 xenograft was transplantable. When a small piece of the tumor was transplanted to another SCID mouse, tumor growth was readily seen within 2 weeks (data not shown).

Because Schwann cells originate from the neuroectodermal neural crest, Schwann cell-derived tumors often show immunoreactions to S-100 protein, MBP, and p75<sup>NGFR</sup>.<sup>15–18</sup> Immunostaining with an anti-S-100 antibody showed that tumor cells from the HMS-97 xenograft strongly and diffusely expressed S-100 protein (Fig. 3A). Similarly, HMS-97 tumor cells also stained robustly for MBP expression (Fig. 3B). The staining for p75<sup>NGFR</sup> expression was weak but detectable (Fig. 3C).

Collectively, these results are consistent with previous reports that malignant schwannomas are transplantable and their Schwann cell characteristics were maintained after xenotransplantation.<sup>12,13</sup> Our study further

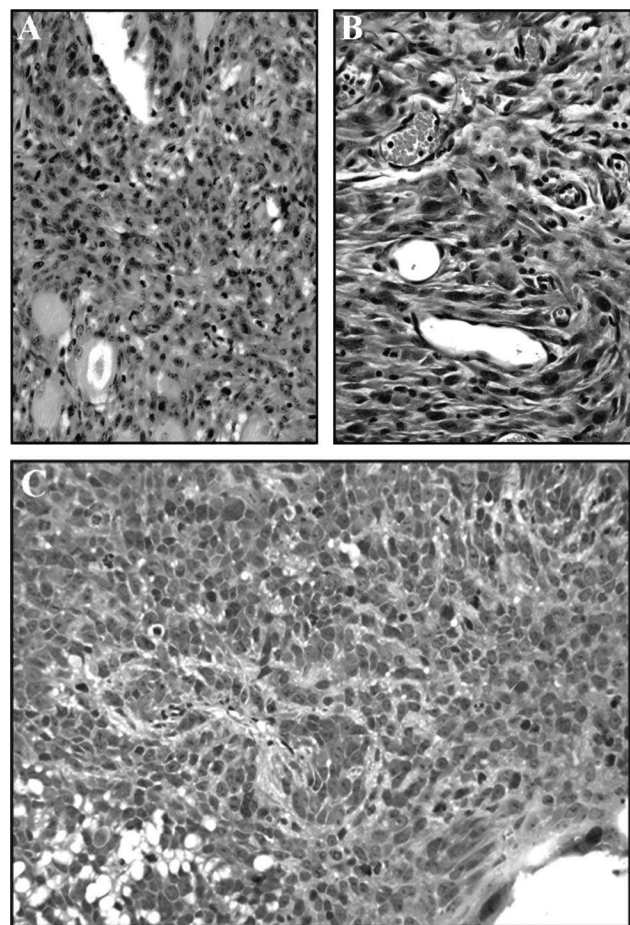


Fig. 2. Histologic analysis of malignant schwannoma xenografts. Malignant-appearing cells with plump, pleomorphic nuclei and densely stained chromatin were present in both the (A) KE-F11 and (B) RT4 tumors. Numerous vascular channels in the RT4 tumor suggest significant tumor angiogenesis. Similarly, malignant-appearing cells with multiple mitotic figures and a high nucleus to cytoplasm ratio were seen in the HMS-97 tumor (C).

demonstrates the feasibility of using MRI to detect the phenotype and growth characteristics of schwannomas in SCID mice. The KE-F11 and HMS-97 xenografts engender malignant solid schwannomas, whereas the RT4 cells produce distinct cystic tumors.

Human VS xenografts persisted for a long period of time and some showed growth in SCID mice. To evaluate potential growth characteristics of human VS, freshly removed tumors were implanted in the thigh of SCID mice. High-field MRI was used to visualize and quantify all VS xenografts in mice as described previously. Analysis of images obtained from each animal at various times after xenotransplantation revealed that the majority of VS xenografts persisted but did not show significant growth (Fig. 4). Most tumor volumes were either unchanged or reduced over the study period. The tumor with the most reduction diminished to about half its original tumor volume over 6 months. It is important to note that even without growth, the xenograft was detectable by MRI scans (Fig. 4A). We were able to maintain one VS xenograft for 13 months until the

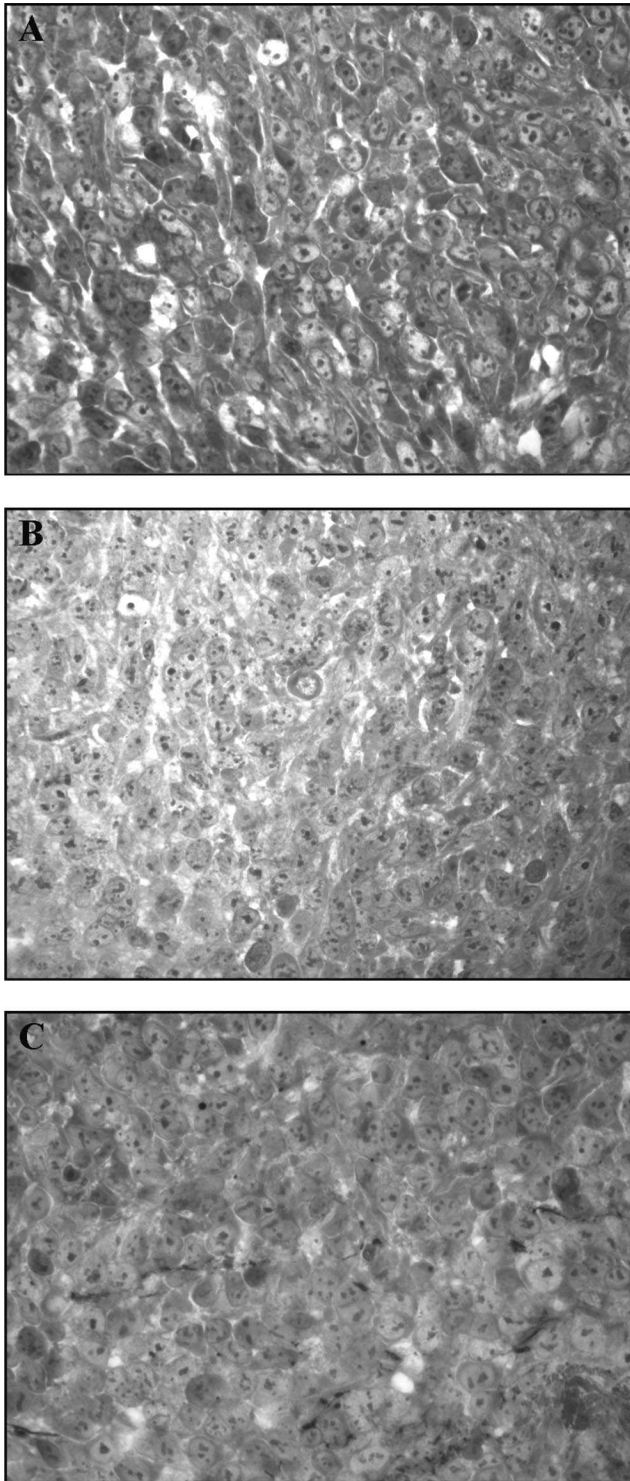


Fig. 3. Immunohistochemical analysis of the HMS-97 xenograft demonstrating continued Schwann cell lineage of tumor cells. Tissue sections containing tumor cells were immunostained with (A) anti-S-100, (B) anti-MBP, and (C) anti-p75<sup>NGFR</sup> antibodies. The positively stained tissue appeared brown. All negative controls did not stain (not shown).

animal was killed for histopathologic examination (see subsequently). We also detected an increase in tumor volume in two of 15 VS xenografts over 6 months (Fig.

4B, 4C). One showed a 60% increase in tumor volume, whereas the other grew to 14 times its original volume.

Representative MRIs from the mouse with the VS xenograft whose tumor volume diminished by approximately half over 6 months are shown in Figure 4A. Although the tumor was small and its size decreased over the study period, a persistent mass could be found at the surgical implant site (arrows) in all images obtained. Because this tumor was surrounded by fatty tissue, both T1- and T2-weighted images depicted the tumor. The post-contrast study at month 6 showed only weak marginal enhancement (Fig. 4A, right column).

When similar MRI sequences were performed on the VS xenograft showing significant growth, changes in tumor growth could be easily seen from both the T1- and T2-weighted images (Fig. 4B). Visual comparison of the images obtained at 1 and 2 months postimplantation revealed that the xenograft became larger. By 6 months, the tumor grew so much that it created an obvious asymmetry in the left implanted thigh. T1-weighted, postcontrast images most clearly outlined the tumor and its growth into the adjacent muscle tissue. Together with the T2 scan, these images confirmed the growth of the VS xenograft.

Histopathologic analysis was performed on the mouse with significant tumor growth to confirm that the mass seen on the MRI was in fact schwannoma tissue by phenotype. Gross examination revealed a large globoid mass in the implanted thigh with no sign of metastasis. Histologically, the tumor was encapsulated and consisted of spindle-shaped cells. Alternating compact areas of elongated cells with occasional nuclear palisading (Antoni A pattern) and less cellular, loosely textured Antoni B areas were seen (Fig. 5A). The tumor cells had relatively abundant cytoplasm with discernible cell margins. All of these characteristics were consistent with a primary benign human VS. We also detected strong immunoreactivity to S-100, p75<sup>NGFR</sup>, and MBP antigens in the area containing tumor cells (Fig. 6A–C).

Similarly, we performed a histopathologic examination on the mouse with a VS implant present but without any growth for 13 months. The xenograft tissue could still be detected by MRI (data not shown) and macroscopic analysis confirmed the presence of a small tumor within the implanted region. Microscopically, the tumor was composed of both ovoid and spindle-shaped cells with foci of lipid laden tumor cells characteristic of an aged vestibular schwannoma (Fig. 5B). Similar to those detected in the VS tumor showing significant growth, strong immunoreactivity, to S-100 and p75<sup>NGFR</sup> proteins was found in the area containing the tumor cells (Fig. 6D, E).

Taken together, these results show that VS xenografts can persist or grow in SCID mice and are readily detectable and quantified by MRI. The tumors retained their original microscopic and immunohistochemical characteristics after prolonged implantation.

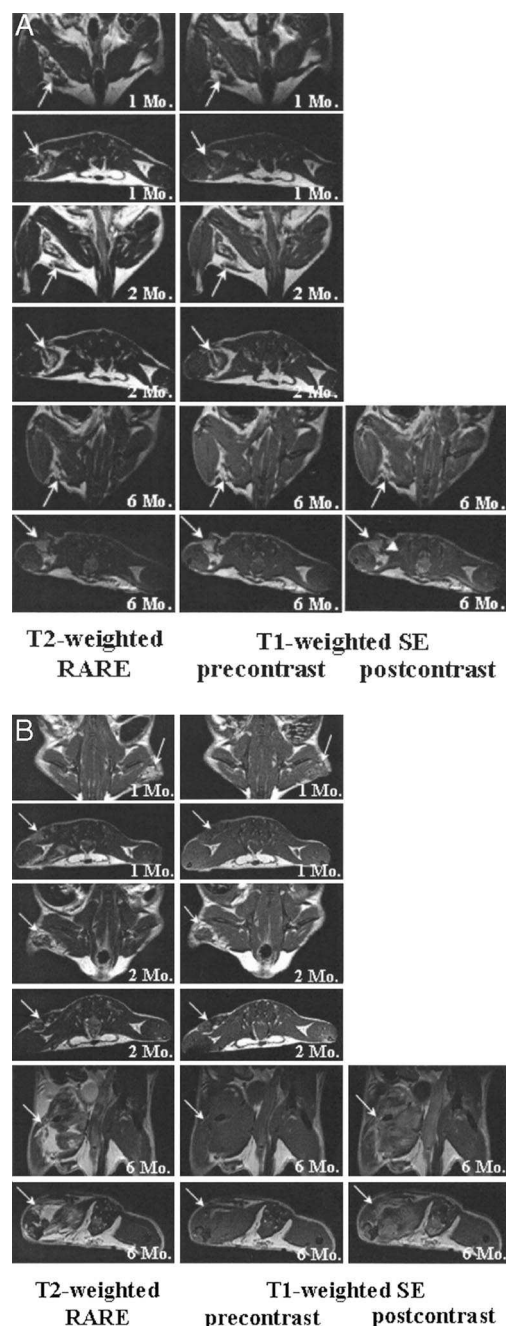
## DISCUSSION

Meaningful translational research in chemotherapy requires disease-specific, reproducible, quantifiable, and cost-effective animal models. Mice have been an attractive species for such models because they can be bred to have little



genetic variability and are accessible to genetic manipulation. Over the past decade, most of the *in vivo* research with schwannomas has focused on *Nf2* transgenic and knockout mice.<sup>16,17</sup> Although soft tissue, peripheral nerve, and central nervous system schwannomas have developed in these animals, no mouse to date has engendered a primary schwannoma on its eighth cranial nerve. Additionally, the conditional *Nf2* mutant mice with schwannomas were found at low frequency only in older mice. Both benign and malignant schwannomas have been found in these mice. This is in contrast to the clearly benign phenotype of VS frequently seen in patients with NF2. Although the reason for these differences is not known, basic schwannoma histology and, perhaps, interspecies differences in normal vestibulocochlear nerve microanatomy may be considered. It should be mentioned that human vestibular bipolar ganglion cells are devoid of myelin sheaths while these cells in rodents are myelinated.<sup>16,17,19</sup> Recently, Stemmer-Rachamimov et al.<sup>20</sup> thoroughly reviewed human and murine schwannomas to create a grading system for these tumors. The World Health Organization describes benign human VS as composed of encapsulated, noninfiltrative tumors composed of mature Schwann cells in Antoni A and Antoni B patterns with Verocay bodies, which are rows of palisading Schwann cell nuclei separated from each other by stroma. The benign schwannomas seen in the *Nf2*-knockout mice were classified as murine genetic engineered mouse I or GEM I tumors because they were most closely related to human VS. Although these benign mouse schwannomas displayed primarily an Antoni A growth pattern with occasional Verocay bodies, they were not encapsulated and were far more infiltrative than human VS. The murine GEM II tumors, which refer to more malignant murine schwannomas, displayed nuclear pleomorphism, increased cellularity, and scattered mitotic figures. These histologic differences between human and mouse schwannomas may make it difficult to directly translate research conclusions drawn from these models to the human disease. For this reason, an alternative model such as the reproducible, quantifiable VS xenograft model that we reported here will be important for translational VS research.

Fig. 4. Quantification of human VS xenografts by magnetic resonance imaging. (A) T2-weighted (left), pre- (middle), and postcontrast T1-weighted images (right) of a vestibular schwannoma (VS) xenograft showed that the tumor persisted in the severe combined immunodeficiency mouse over the 6-month study period. The first coronal and axial magnetic resonance imaging scans were performed 1 month after surgery to ensure that the animals had healed. Follow-up magnetic resonance images were obtained at the 2- and 6-month time points. Note that the tumor is readily visible in a fatty tissue pocket between the thigh musculature on both T1 and T2 images (arrows). T1 post-contrast images obtained at 6 months show some enhancement at the tumor margins (arrowhead). (B) T2-weighted (left), pre- (middle), and postcontrast T1-weighted images (right) of a VS xenograft demonstrating significant growth over a 6-month period. Note that the tumor (arrow) appears larger on the 2-month images. T2-weighted imaging at 6 months showed that the tumor extended into the surrounding muscles. Postcontrast T1-weighted images verified the presence of tumor within the thigh musculature. (C) Volumetric measurement of 15 VS xenografts over a 6-month period. Note that most tumors remained stable or regressed slightly, whereas two xenografts demonstrated significant growth.



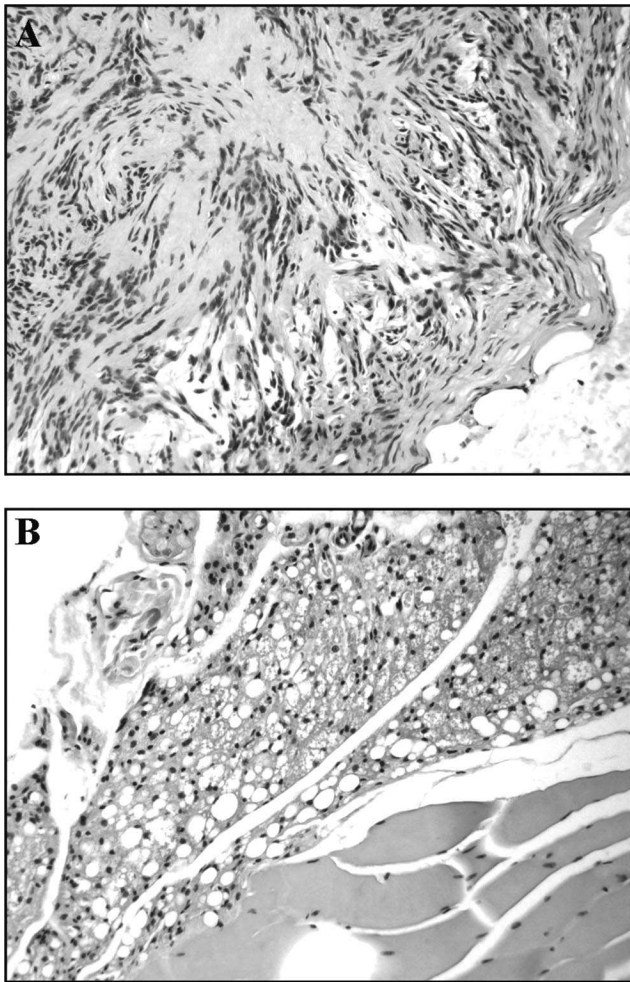


Fig. 5. Histologic analysis of the human vestibular schwannoma (VS) xenografts in severe combined immunodeficiency mice. (A) A tissue section of a VS xenograft harvested 6 months after implantation demonstrated significant tumor growth. The encapsulated tumor mass consisting of spindle cells with no significant atypia and palisading nuclei in Antoni A and Antoni B configurations, all of which are histologic characteristics of benign human VS. (B) A tissue section of a VS xenograft 13 months postimplantation confirmed the presence of tumor cells within the mass seen on magnetic resonance imaging. Note the cells with bland-appearing homogeneous nuclei and some foci of lipid-laden tumor cells in the specimen characteristic of an aged schwannoma.

We have demonstrated the use of MRI in assessing and quantifying schwannoma xenografts in SCID mice. The technique offers investigators the ability to assess an individual xenograft over time without requiring serial surgery or killing the animal. We showed that MRI reliably visualized both human and rat malignant schwannoma xenografts and distinguished between the solid and cystic tumor phenotypes. Immuno- and histopathologic analyses confirmed the MRI findings. The RT4 xenograft is the first description of an animal model for cystic schwannomas in the literature. Human cystic tumors are clinically aggressive, may grow rapidly, and have poorer outcomes. The unique RT4 xenograft may allow the investigation of the basic science behind cystic schwannomas.

MRI of human VS xenografts revealed that although most VS implants diminished slightly and two grew significantly over time, all of the tumors persisted and could be readily imaged. It is important to note that patients with VS *in situ* demonstrate a similar pattern of disease. Most individuals' tumors persist or grow slowly over time, approximately 5% diminish in size when imaged serially, and approximately 10% grow rapidly.<sup>1</sup> Interestingly, the nongrowing human VS xenografts persisted in SCID mice for 6 to 13 months. We were able to use the high-field MRI to monitor a xenograft for 13 months. Histologically, the persistent xenograft retained characteristics of an aged vestibular schwannoma. In most of the animals imaged over a 6-month period, the variance in tumor volumes was limited. Defining the variance more precisely would require a larger cohort of animals imaged over a 1-year time period. Once established, deviations from the expected variance could be used for evaluating growth-inhibiting effects of potential chemotherapeutic interventions.

The gold standard for evaluating human VS *in situ* is T1-weighted MRI with gadolinium enhancement.<sup>1</sup> This technique provides sharp contrast between the tumor and surrounding fluid spaces and neural structures. Our MRI analysis of VS xenografts also suggests that T1 postcontrast images best delineate the tumor margins and contrast can be adequately delivered to the mouse using tail vein catheter injections. However, this technique is not without risk to the animal. The volume of gadolinium along with the flush of saline that follows can fluid overload the animal and increase its mortality risk. We have found that T2-weighted RARE images may adequately delineate the xenografts margins and allow for volumetric measurements. Thus, the injection of contrast agent is used in those tumors that are difficult to differentiate from adjacent thigh musculature.

Most human VS tumors are slow growing, whereas only a few proliferate rapidly.<sup>1</sup> Tumor genetics may play a role in the growth potential of these benign tumors. Mutations in the *NF2* gene have been detected in NF2-associated VS, sporadic VS, and cystic schwannomas.<sup>6</sup> Several attempts have been made to correlate clinical expression and specific *NF2* mutations in VS and other NF2-associated tumors. Initially, mutations that cause truncation of the *NF2* protein were reported to cause a more severe phenotype, whereas missense mutations or small in-frame insertions correlated with a mild phenotype. However, there have been reports of severe phenotypes associated with missense mutations in the *NF2* gene, and likewise, large deletions have been reported to give rise to mild phenotypes. In addition, phenotypic variability within NF2 families carrying the same germline mutation has been reported. Given this heterogeneity of clinical response to various mutations, it remains vital to identify key regulatory factors involved in the growth of various types of schwannomas.

Research to better understand VS tumorigenesis has been hampered by the lack of a spontaneous VS cell line available for *in vitro* study. VS cells are difficult to culture and have a very limited lifespan *in vitro*. A previous attempt to immortalize VS cells using the human papilloma virus E6–E7 oncogenes yielded the HEI193 cell line with



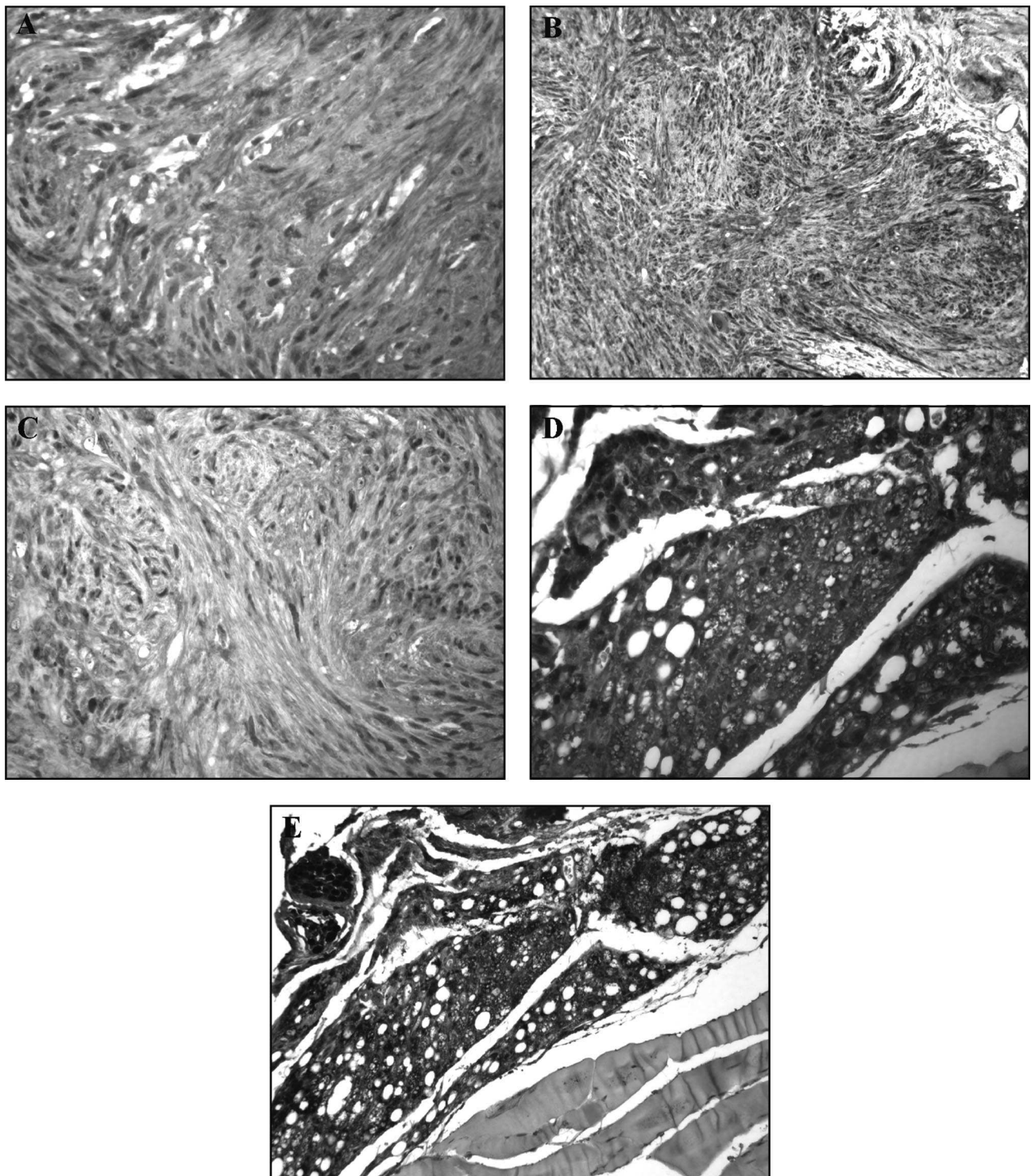


Fig. 6. Immunostained human vestibular schwannoma (VS) xenograft tissue sections. Tissue sections from the VS xenograft showing significant growth over a 6-month period were stained with antibodies to (A) S-100, (B) MBP, and (C) p75<sup>NGFR</sup>. Similarly, sections from a VS xenograft that did not grow but persisted in the mouse for 6 months were stained with (D) anti-S-100 and (E) anti-p75<sup>NGFR</sup> antibodies. These VS xenografts retained positive immunoreactivity to these Schwann cell markers, whereas the adjacent nontumor cells showed no staining.

altered growth properties such as morphologic changes and independence of Schwann cell growth factors.<sup>21</sup> The fact that some VS xenografts grow in SCID mice and may be transplantable suggests that they may be used as a

means to enhance the growth potential of VS cells in culture. By transplanting the growing VS tissue repeatedly through mice, VS cells with enhanced growth capability may be isolated and used to establish a VS cell line.

In summary, this study established a quantifiable human VS xenograft model in SCID mice that uses MRI to measure tumor volumes. VS xenografts demonstrate biologic variability in their growth potential, but although individual grafts may grow, persist, or regress over time, MRI successfully quantifies these tumors noninvasively. VS xenografts represent a model complimentary to *Nf2* transgenic and knockout mice for translational research and improved drug screening.

## Acknowledgments

The authors thank Dan Scoles for the RT4 cell line, Peter Wassenaar and Abdulkarim Eroglu for technical assistance, and Sarah S. Burns for critical reading of the manuscript. Mark Lorenz was a recipient of the Young Investigator Award from the Children's Tumor Foundation.

## BIBLIOGRAPHY

1. Neff BA, Welling DB, Akhmametyeva E, Chang L-S. The molecular biology of vestibular schwannomas: dissecting the pathogenic process at the molecular level. *Otol Neurotol* 2006;27:197–208.
2. Rouleau GA, Merel P, Lutchman M, et al. Alteration in a new gene encoding a putative membrane-organising protein causes neurofibromatosis type 2. *Nature* 1993;363:515–521.
3. Trofatter JA, MacCollin MM, Rutter JL, et al. A novel Moesin-, Exrin-, Radixin-like gene is a candidate for the neurofibromatosis 2 tumor-suppressor. *Cell* 1993;72:791–800.
4. Charabi S, Klinken L, Tos M, Thomsen J. Histopathology and growth pattern of cystic acoustic neuromas. *Laryngoscope* 1994;104:1348–1352.
5. Fundova P, Charabi S, Tos M, Thomsen J. Cystic vestibular schwannoma: surgical outcome. *J Laryngol Otol* 2000;114:935–939.
6. Welling DB, Lasak JM, Akhmametyeva EM, Chang L-S. cDNA microarray analysis of vestibular schwannomas. *Otol Neurotol* 2002;23:736–748.
7. Shin M, Ueki K, Kurita H, Kirino T. Malignant transformation of a vestibular schwannoma after gamma knife radiosurgery. *Lancet* 2002;360:309–310.
8. Niemczyk K, Vaneecloo FN, Lecomte MH, et al. Correlation between Ki-67 index and some clinical aspects of acoustic neuromas (vestibular schwannomas). *Otolaryngol Head Neck Surg* 2000;123:779–783.
9. Lee JK, Sobel RA, Chiocca EA, Kim TS, Martuza RL. Growth of human acoustic neuromas, neurofibromas and schwannomas in the subrenal capsule and sciatic nerve of the nude mouse. *J Neurooncol* 1992;14:101–112.
10. Charabi S, Rygaard J, Klinken L, Tos M, Thomsen J. Subcutaneous growth of human acoustic schwannomas in athymic nude mice. *Acta Otolaryngol* 1994;114:399–405.
11. Stidham KR, Roberson JB Jr. Human vestibular schwannoma growth in the nude mouse: evaluation of a modified subcutaneous implantation model. *Am J Otol* 1997;18:622–626.
12. Yamate J, Yasui H, Benn SJ, et al. Characterization of newly established tumor lines from a spontaneous malignant schwannoma in F344 rats: nerve growth factor production, growth inhibition by transforming growth factor- $\beta$ 1, and macrophage-like phenotype expression. *Acta Neuropathol (Berl)* 2003;106:221–233.
13. Imada M, Sueoka N. Clonal sublines of rat neurotumor RT4 and cell differentiation. I. Isolation and characterization of cell lines and cell type conversion. *Dev Biol* 1978;66:97–108.
14. John MR, Wickert H, Zaar K, et al. A case of neuroendocrine oncogenic osteomalacia associated with a PHEX and fibroblast growth factor-23 expressing sinusoidal malignant schwannoma. *Bone* 2001;29:393–402.
15. Charabi S, Simonsen K, Charabi B, et al. Nerve growth factor receptor expression in heterotransplanted vestibular schwannoma in athymic nude mice. *Acta Otolaryngol* 1996;116:59–63.
16. Giovannini M, Robanus-Maandag E, Niwa-Kawakita M, et al. Schwann cell hyperplasia and tumors in transgenic mice expressing a naturally occurring mutant NF2 protein. *Genes Dev* 1999;13:978–986.
17. Giovannini M, Robanus-Maandag E, van der Valk M, et al. Conditional biallelic Nf2 mutation in the mouse promotes manifestations of human neurofibromatosis type 2. *Genes Dev* 2000;14:1617–1630.
18. Hung G, Colton J, Fisher L, et al. Immunohistochemistry study of human vestibular nerve schwannoma differentiation. *Glia* 2002;38:363–370.
19. Ona A. The mammalian vestibular ganglion cells and the myelin sheath surrounding them. *Acta Otolaryngol Suppl* 1993;503:143–149.
20. Stemmer-Rachamimov AO, Louis DN, Nielsen GP, et al. Comparative pathology of nerve sheath tumors in mouse models and humans. *Cancer Res* 2004;64:3718–3724.
21. Hung G, Li X, Faudoa R, et al. Establishment and characterization of a schwannoma cell line from a patient with neurofibromatosis 2. *Int J Oncol* 2002;20:475–482.